Stability of vacancy clusters in FeCr alloys: A study of the Cr concentration dependence

Jesús M. Sampedro , Emma del Rio , María J. Caturla , Alfredo Caro , Magdalena Caro , J. Manuel Perlado

A B S T R A C T

Fe–Cr based alloys are the leading structural material candidates in the design of next generation reactors due to their high resistance to swelling and corrosion. Despite these good properties there are others, such as embrittlement, which require a higher level of understanding in order to improve aspects such as safety or lifetime of the reactors. The addition of Cr improves the behavior of the steels under irradiation, but not in a monotonic way. Therefore, understanding the changes in the Fe–Cr based alloys microstructure induced by irradiation and the role played by the alloying element (Cr) is needed in order to predict the response of these materials under the extreme conditions they are going to support. In this work we perform a study of the effect of Cr concentration in a bcc Fe–Cr matrix on formation and binding energies of vacancy clusters up to 5 units. The dependence of the calculated formation and binding energy is investigated with two empirical interatomic potentials specially developed to study radiation damage in Fe–Cr alloys. Results are very similar for both potentials showing an increase of the defect stability with the cluster size and no real dependence on Cr concentration for the binding energy.

1. Introduction

High-Cr ferritic/martensitic steels are leading structural candidates for advanced fission reactors, accelerator-driven systems using spallation neutron sources and fusion reactors for the range of operational temperatures below 550 °C [1–3]. The high resistance to radiation effects added to the better resistance against corrosion for high chromium contents is the main cause for this [4–9]. However, these alloys present problems of irradiation embrittlement [10–13]. In addition, these materials should be able to withstand high irradiation doses and temperatures which will change the microstructure with time. Therefore, in order to have the best composition and to predict the evolution in time of microstructure of these materials as better as possible to have longer service lifetime and keep high safety conditions in future nuclear plants, we need to obtain the best understanding of their behavior to neutron irradiation in aggressive environments. One of the important factors that require a better understanding to predict the change in the ferritic/martensitic steels properties with radiation is how they are affected by the increase of Cr concentration in the material. It is known that the addition of Cr improves the performance of the steels under irradiation [5,6,10,11,14–21], but not in a monotonic way. Several studies, both simulation and experimental [15,21–29], have been performed but the effect of Cr content continues without being completely understood.

In this article we present a comparative study between two empirical interatomic potentials of the effect of Cr content on the stability of vacancy cluster defects. Formation and binding energies of clusters up to five defects have been calculated. The aim of this work is to obtain a better understanding of the effect of Cr on the properties of the alloy at a fundamental level, but also answer fundamental questions such as the dependence of defect formation energies on Cr concentration which could help in the development of object kinetic Monte Carlo models for alloys under irradiation. Results from object kinetic Monte Carlo models could be directly compared to experimental measurements.

The paper is arranged as follows. In the next section we describe the methodology used. A detailed analysis and discussion of the results is presented in Section 3. And finally, a summary and conclusions are formulated in Section 4.

2. Methodology

Calculations have been performed with two different interatomic empirical potentials in order to compare the results and

to study the possible dependence of these results on the potential employed. One of these two potentials, hereon 2BM potential, is based on the two-band model formalism with the mixing enthalpy obtained with the projector augmented wave method (PAW) [30]. The other potential, here on CDM potential, is created introducing an explicit dependence on concentration [31]. The new version of this latest potential, specially modified to study radiation damage defects in Fe–Cr alloys [32] and tested in previous works [32,33] is used.

The calculations were performed at constant volume, relaxing the atomic positions by using the conjugate gradient algorithm [34]. Periodic boundary conditions were set for all the calculations. The lattice parameter employed is 2.855 Å for bcc Fe and both potentials, which presents a very good agreement with the experimental value of 2.867 Å [35,36], and is changed as a function of Cr content for all the concentrations studied (0%, 1%, 5%, 10% and 15%) (see Table 1). Formation energies have been calculated for cell sizes of 2000 atoms in the case of the perfect cell and (2000 – m), where m is the number of defects in the cluster, for the vacancy clusters, if not otherwise mentioned.

The formation energy of an m vacancy cluster, E_f, with n Fe atoms and p Cr atoms removed to build the vacancy cluster, is given by

$$E_f = E_{defect} - [E_{without\ defect} - nE(Fe) - pE(Cr) - \Delta h] \quad (1)$$

where E_{defect} is the energy of the system with the defect, $E_{without\ defect}$ is the energy of the system without the defect, E[Fe] and E[Cr] are the energies per atom of the bcc Fe and bcc Cr lattices respectively and Δh is the change in enthalpy between the systems without and with the defect. The difference in enthalpy is calculated as:

$$\Delta h = NH_{mix}(X_{without\_defect}) - (N-m)H_{mix}(X_{with\_defect}) \quad (2)$$

where N is the total number of atoms in the simulation cell, H_{mix} is the mixing enthalpy and $X_{without\_defect}$ and X_{with_defect} are the Cr concentrations in the cell without and with the defect respectively. The mixing enthalpy is obtained from the following polynomial fits for each of the two potentials:

$$H_{mix}{}^{2BM}(X) = (-0.0001551 - 0.2631X + 4.8283X^2 - 20.4868X^3 + 32.676X^4) \quad (3)$$

$$H_{mix}{}^{CDM}(X) = (-0.00003732 - 0.1570X + 3.2818X^2 - 9.3996X^3 + 8.6432X^4) \quad (4)$$

This term, Δh, is included to take into account the different in concentration due to the presence of the vacancy cluster.

The binding energy of a cluster of size m, E_b, is defined as the difference between the sum of the formation energies of one vacancy, $E_f(a)$, and the formation energy of the $(m-1)$ vacancy cluster, $E_f(b)$, minus the formation energy of the m vacancy cluster, $E_f(ab)$. The binding energy then becomes

$$E_b = E_f(a) + E_f(b) - E_f(ab) \quad (5)$$

Table 1
Lattice parameter values (A) as a function of Cr concentration calculated with the 2BM and CDM potentials.

%Cr	2BM A (Å)	CDM A(Å)
0.00	2.8553	2.8553
0.80	2.8554	2.8555
5.60	2.8570	2.8568
10.00	2.8595	2.8581
15.60	2.8632	2.8596

Positive binding energy means attraction between the defects and reciprocally.

The vacancy cluster formation energy was calculated for a series of samples with increasing Cr concentration. Previously to the study of the effect of Cr concentration on vacancy clusters stability, we have performed calculations to determine the more stable cluster geometry for the clusters under observation, i.e. up to a size of 5 vacancy defects. This study was performed with only four different Cr distributions for all cluster sizes and Cr concentrations. In order to create the $(m+1)$ vacancy cluster, only first nearest neighbor ($1nn$) positions with respect to the m cluster have been taken into account when removing a new atom in the cell. The only exception to this is the $m=2$ cluster where $1nn$ and second nearest neighbor ($2nn$) atoms have been considered as the bibliography [37] suggests the latter geometry as the most stable in pure Fe showing a higher binding energy than the cluster built from $1nn$ atoms.

Once the most stable configuration has been determined, it will be our starting geometry for the systematic study of the cluster formation energy with Cr concentration. Since the local position of the defect with respect to the Cr atoms in substituted positions could influence the formation energy value, we have explored all the possibilities of the cluster position for each concentration and cluster size geometry. These calculations have been performed for cells of 250 atoms.

3. Results and discussion

First of all we have studied the different possible locations of vacancies to create a cluster for all sizes considered. Although only $1nn$ atoms with respect to the $(m-1)$ cluster are considered to be removed for cluster sizes of $m \geqslant 3$, the possibilities grow up to 3 in the case of $m=3$, 12 for $m=4$ and 62 for $m=5$. Formation energies have been calculated for all these possibilities with the two empirical potentials mentioned above, the CDM and the 2BM, and for Cr concentrations of 0%, 1%, 5%, 10% and 15% and 4 different initial Cr distributions in order to find the most stable geometry for each cluster size and concentration.

The most stable geometries for each cluster size shown in Fig. 1, are the same with the two empirical potentials studied and show no dependence on the Cr concentration, i.e. they are the same for all the concentrations studied. This gives us a good first guess of the cluster geometry for our following systematic study. Although on average, the configurations shown in Fig. 1 are the most stable

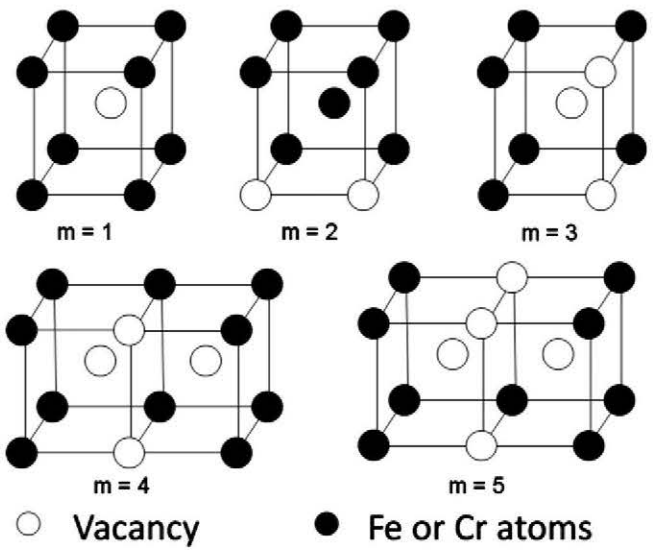

Fig. 1. More stable geometries for vacancy clusters up to 5 defects.

for all the concentrations, there are some cases where geometries with lower energies are found different from those shown in Fig. 1. The number of these configurations that differ from the average increase with the cluster size and Cr concentration and appear more often with the 2BM potential. This could be due to a higher probability of finding Cr atoms in the nearby of the defect with the increase of the Cr content and the cluster size. Previous studies have shown an effect on the formation energy of the defect as a function of 1*nn* and 2*nn* Cr atoms sites [29,32,33].

Formation energy of the clusters shows a slight increase with the Cr content. This can be explained taking into account that the formation energy of 1 vacancy in pure bcc Cr is higher (2.56 eV) than in pure bcc Fe (1.71 eV) [33].

It is also interesting to note that the vacancies in the more stable geometry are always 1*nn* or 2*nn* between them, i.e. the cluster tends to be as compact as possible.

Once the most stable geometry for each cluster size has been determined we have used it to calculate the binding and formation energies of vacancy clusters up to 5 defects. Since the local Cr distribution on the cell has an effect on the defect formation energies, showed in the calculation of the more stable geometries of the vacancy clusters and in previous studies for the vacancy and interstitial defects [32,33], we decided to perform calculations over all the possibilities of the cluster environment. The change in the environment of the cluster is achieved by displacing all the defects in the vacancy cluster along the simulation cell so that in every calculation the cluster is located in a different position, sampling the whole cell. Due to the large number of calculations, the size of the cell was reduced to 250 atoms. Then, we have 250 formation energy values for each cluster size, potential and concentration. Fig. 2 shows the formation energy histograms for the 2BM potential (upper half of the figure) and the CDM potential (bottom half of the figure) for $m = 1$ and 1% Cr (Fig. 2a), $m = 1$ and 15% Cr (Fig. 2b), $m = 5$ and 1% Cr (Fig. 2c) and $m = 5$ and 15% Cr (Fig. 2d). For $m = 1$ and 1% Cr, most of the cases give a formation energy value very similar to that of the vacancy in pure bcc Fe. However, there are a few cases where the formation energy is slightly higher. The analysis of these configurations shows that they have more than 1 Cr atoms in the nearby of the vacancy (1*nn* or 2*nn* sites). The effect of having configurations with higher formation energy increases with the Cr concentration. Therefore, the formation energy increases slightly with the concentration. Also, it can be observed a greater dispersion in the values of the formation energy with higher Cr contents. A similar behavior is shown with the size of the cluster: the dispersion increases with the size of the cluster. This can be explained in terms of possibilities of having Cr atoms nearby. As higher Cr concentrations or cluster sizes provide more possibilities of having Cr atoms at 1*nn* or 2*nn* positions, the dispersion in the value of the formation energy increases. Fig. 2a–d show similar values for both potentials, although a larger range of energy values is observed for the CDM potential, indicating a greater sensitivity to local Cr distribution for this potential which was also previously reported in the formation energy of cells with substitutional Cr clusters of $m = 2$, 3 or 4 Cr atoms [33]. All these effects: greater dispersion in the values with the Cr content, higher dispersion with the CDM potential and higher formation energy with the Cr concentration, are observed more clearly as the cluster size grows. Also, as the Cr concentration increases, there is a bigger difference between CDM and 2BM formation energy values.

From all the above values, we have calculated the average formation energy as a function of the concentration for each cluster size. Fig. 3 shows the formation energy of the monovacancy (Fig. 3a) and cluster with 5 vacancies (Fig. 3b) with the Cr content. It can be seen in this fig. that the formation energy increases with

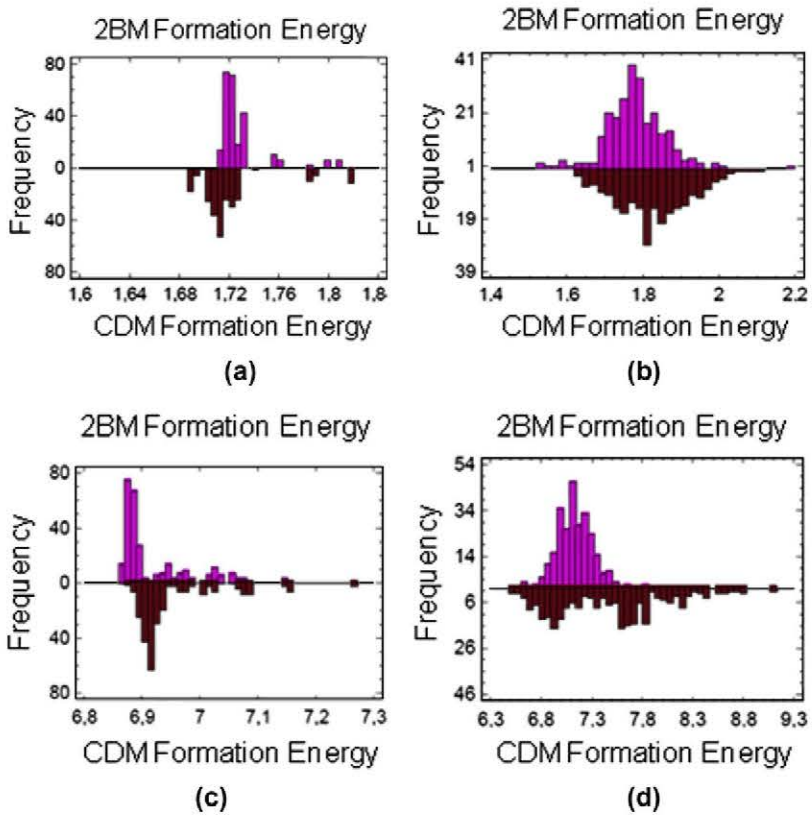

Fig. 2. Vacancy cluster formation energy histograms for different cluster sizes and Cr concentrations. (a) 1 vacancy and 1% Cr, (b) 1vacancy and 15% Cr, (c) 5 vacancies and 1% Cr, (d) 5 vacancies and 15% Cr.

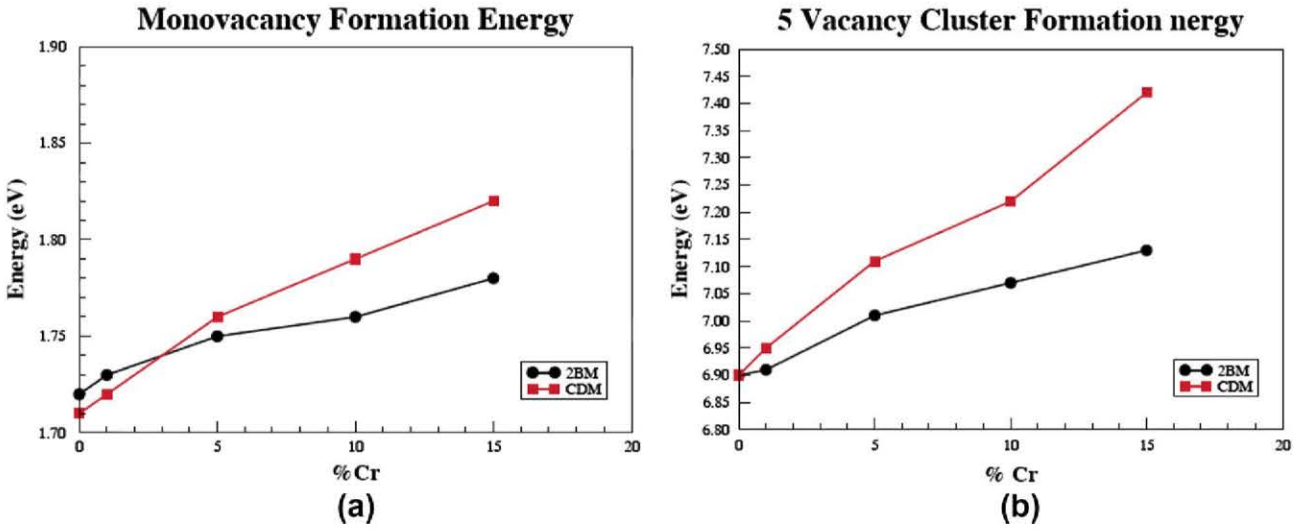

Fig. 3. Vacancy cluster formation energy as a function of Cr concentration for different cluster sizes (m): (a) $m = 1$ and (b) $m = 5$.

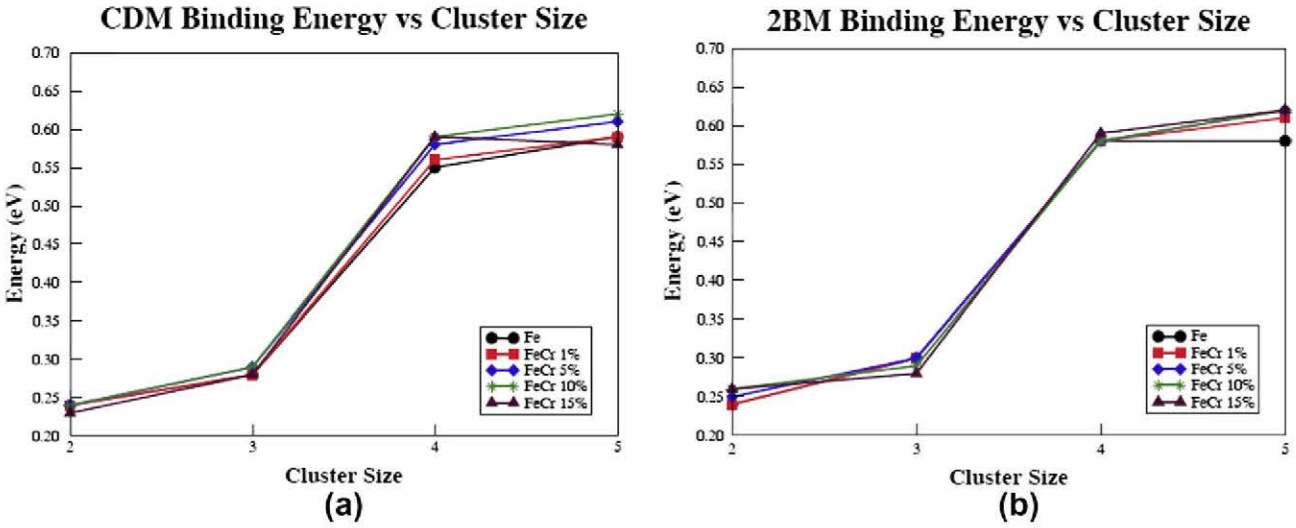

Fig. 4. Vacancy cluster binding energy as a function of Cr concentration calculated with (a) CDM potential and (b) 2BM potential.

the cluster size and the Cr concentration and it occurs in the same way for both potentials and cluster sizes. CDM potential predicts higher formation energies than the 2BM potential and the differences between CDM and 2BM values are greater for higher Cr concentrations. Also, differences in the energy between the larger and lower concentrations are smaller with the 2BM potential, i.e. the change in the formation energy with Cr concentration is smaller with the 2BM potential than with the CDM potential. For example, $E_f(15\%\ \mathrm{Cr}) - E_f(1\%\ \mathrm{Cr}) = 0.3$ eV for the CDM and only 0.14 eV for the 2BM for clusters of size $m = 3$, indicating again a higher sensitivity of the CDM potential to the Cr content.

Finally, from the average formation energy we have calculated the binding energy for each cluster size and concentration. Fig. 4 shows the binding energy as a function of the cluster size for different Cr concentrations and calculated with the CDM potential (Fig. 4a) and with the 2BM potential (Fig. 4b). Very similar results are obtained for the binding energy with both potentials. And all of them are positive, indicating attraction between the components of the cluster. The binding energy increases with the cluster size. Small increases in the binding energy are observed for 3 and 5 vacancy clusters with respect to the 2 and 4 vacancy clusters respectively. But there is a change in the binding energy of ~0.3 eV when the size of the cluster increases from $m = 3$ to $m = 4$. On the other hand, whereas a little difference which increases with the Cr concentration and the size of the cluster was observed in the formation energies, the binding energy is the same for both potentials and shows no dependency on the Cr concentration. This is due to the fact that the formation energy increases linearly with the Cr concentration and there is a cancellation of effects as the effect of Cr for a m cluster is m times the effect for 1 vacancy.

4. Summary and conclusions

We present a detailed study of the influence of Cr concentration for vacancy clusters up to 5 defects. This study has been performed with two empirical potentials, the CDM and the 2BM, and for 0%, 1%, 5%, 10% and 15% Cr. First, the most stable geometry for each cluster size and concentration has been studied and using these geometries, formation and binding energies have been calculated.

Both potentials predict an increase of the formation energy with the Cr concentration and the cluster size. Also, the range of values

obtained increase with the Cr concentration and the cluster size reflecting the influence of the Cr local distribution. This effect is more pronounced in the case of the CDM potential which means that this potential is more sensitive to Cr-Cr interactions. CDM predicts higher formation energy values than 2BM and the differences between the values calculated with both potentials increase with the Cr content. Nevertheless binding energies are very similar for both potentials and they are almost the same for all the concentrations studied and for pure bcc Fe showing no Cr dependence of the binding energy on the Cr content. This is due to a cancellation of the Cr effect as for vacancy clusters of size m it is m times the effect for 1 vacancy.

This work has been partially supported by the European Commission within the FP7 project GETMAT (Grant agreement number 212175) and HiPER (Grant agreement number 211737. FP7-INFRASTRUCTURES-2007-1), the VI Spanish National Project ENE2008-06403-C06-06, the European Union Keep in Touch Program on Inertial Confinement Fusion (ref. 08/061), and the European Fusion Development Agreement (EFDA). A.C. and M.C. acknowledge support from the Los Alamos's Laboratory Directed Research and Development Program. AC also acknowledges support from the DOE's Energy Frontier Research Center (EFRC) for Materials under Irradiation and Mechanical Extremes.This work also contributes to the International Atomic Energy Agency CRP SMoRE program. Thanks to CeSViMa for computational support.

L.K. Mansur, A.F. Rowcliffe, R.K. Nanstad, S.J. Zinkle, W.R. Corwin, R.E. Stoller, J. Nucl. Mater. 329–333 (2004) 166.
E.A. Little, Mater. Sci. Technol. 22 (2006) 491.
R.L. Klueh, A.T. Nelson, J. Nucl. Mater. 371 (2007) 37.
M.L. Jenkins, C.A. English, B.L. Eyre, Philos. Mag. A 38 (1978) 97.
E.A. Little, D.A. Stow, J. Nucl. Mater. 87 (1979) 25.
E.A. Little, R. Bullough, M.H. Wood, Proc. R. Soc. Lond. A (1980) 372.
F.A. Garner, M.B. Toloczko, B.H. Sencer, J. Nucl. Mater. 276 (2000) 123.
A. Fry, S. Osgerby, M. Wright, National Physics Laboratory Report NPL MATC(A) (2002) 90.
R. Lindau, A. Möslang, M. Schirra, Fus. Eng. Des. 61–62 (2002) 659.
H. Kayano, A. Kimura, M. Narui, Y. Sasaki, Y. Suzuki, S. Ohta, J. Nucl. Mater. 155–157 (1988) 978.
A. Kohyama, A. Hishinuma, D.S. Gelles, R.L. Klueh, W. Dietz, K. Ehrlich, J. Nucl. Mater. 233–237 (1996) 138.
E. Lucon, Annual Report 2004 EURATOM-Belgian State Association, 2004, p. 14.
T. Yamamoto, G.R. Odette, H. Kishimoto, J.W. Rensman, P. Miao, J. Nucl. Mater. 356 (2006) 27.
E.A. Little, D.A. Stow, J. Mater. Sci. 14 (1980) 89.
S.I. Porollo, A.M. Dvoriashin, A.N. Vorobyev, Yu.V. Konobeev, J. Nucl. Mater. 256 (1998) 247.
Yu.V. Konobeev, A.M. Dvoriashin, S.I. Porollo, F.A. Garner, J. Nucl. Mater. 355 (2006) 124.
D.S. Gelles, J. Nucl. Mater. 108–109 (1982) 515.
Y. Katoh, A. Kohyama, D.S. Gelles, J. Nucl. Mater. 225 (1995) 154.
D.S. Gelles, J. Nucl. Mater. 225 (1995) 163.
F. Maury, P. Lucasson, A. Lucasson, et al., J. Phys.: Met. Phys. 17 (1987) 1143.
A.L. Nikolaev, J. Phys.: Condens. Mat. 11 (1999) 8633.
K. Arakawa, M. Hatanaka, H. Mori, K. Ono, J. Nucl. Mater. 329–333 (2004) 1194.
D.A. Terentyev, L. Malerba, A.V. Barashev, Phil. Mag. Lett. 85 (2005) 587.
D.A. Terentyev, P. Olsson, L. Malerba, A.V. Barashev, J. Nucl. Mater. 362 (2008) 167.
D.A. Terentyev, A.V. Barashev, L. Malerba, Phil. Mag. 88 (2008) 21.
A.L. Nikolaev, V.L. Arbuzov, A.G. Davletshin, J. Phys.: Condens. Matter 9 (1997) 4385.
P. Olsson, C. Domain, J. Wallenius, Phys. Rev. B 75 (2007) 014110.
T.P.C. Klaver, P. Olsson, M.W. Finnis, Phys. Rev. B 76 (2007) 214110.
A. Froideval, R. Iglesias, M. Samaras, S. Schuppler, P. Nagel, D. Grolimund, M. Victoria, W. Hoffelner, Phys. Rev. Lett. 99 (2007) 237201.
P. Olsson, J. Wallenius, C. Domain, K. Nordlund, L. Malerba, Phys. Rev. B 72 (2005) 214119.
A. Caro, D.A. Crowson, M. Caro, Phys. Rev. Lett. 95 (2005) 075702.
E. del Rio, J.M. Sampedro, H. Dogo, M.J. Caturla, M. Caro, A. Caro, J.M. Perlado, J. Nucl. Mater. 408 (2011) 18–24.
J.M. Sampedro, E. del Rio, M.J. Caturla, M. Victoria, J.M. Perlado, J. Nucl. Mater. 417 (2011) 1050.
Numerical Recipes in Fortran 77, second ed. (1992) 413.
C. Kittel, Introduction to Solid State Physics, seventh ed., Wiley, New York, 1996.
R. Kohlaas, P. Donner, N. Schmitz-Praughe, Z. Angew. Phys. 23 (1967) 245.
L. Malerba, M.C. Marinica, N. Anento, C. Björkas, H. Nguyen, C. Domain, F. Djurabekova, P. Olsson, K. Nordlund, A. Serra, et al., J. Nucl. Mater. 406 (2010) 19.